Use of Thermal Isolation to Improve Thermoelectric System Operating Efficiency

Lon E. Bell
BSST LLC
5462 Irwindale Avenue
Irwindale, CA 91706
lbell@amerigon.com; 626-815-7430

Abstract

Thermal isolation of sections of individual thermoelectric elements, modules and arrays of modules can be used to progressively heat and cool a working fluid so as to increase system efficiency when compared with that of standard TE modules with isothermal hot and cold sides. Equations for performance in heating and cooling modes are derived for steady state conditions with one-dimensional, temperature-independent material properties. Analytical approximations with closed form solutions are given for COP in cooling and heating. Results are compared with precise numerical solutions. Efficiency is shown to increase up to 120% over that of conventional TE modules for certain important applications that involve cooling or heating of a fluid or solid, such as air conditioning and heating. Limitations of the technology are also discussed. It is shown that in the particular case of steady state refrigeration usage benefit is limited or does not occur. Predicted performance of air conditioning systems using thermal isolation, in combination with advanced TE materials with *ZT* of 2 to 3 are shown to be comparable to refrigerant 134A.

Introduction

The broader use of solid-state energy converters (SSECs) is hampered by the thermodynamic efficiency exhibited by present systems. The most widely pursued approach to resolving the deficiency is through the improvement of basic energy conversion materials. Significant efforts by DARPA, DOE and ONR have led to advancements that show great promise. Results by Venkatasubramanian [1], Harman [2], and possible improvements by others [3, 4, 5, 6] represent significant steps and appear to enable about a doubling of efficiency of today's standard Bi Te thermoelectric materials. A second approach has been the enhancement of the performance of solid-state energy converters through material processing [7], design optimization for specific applications [8], and the use of ancillary components and materials such as higher thermal conductivity fluid systems [9] and heat pipes [12]. The results of these efforts have been gradual performance increase, totaling about 30%, over the last five decades.

A third approach to improvement is through the development of alternative thermodynamic operating cycles. Such efforts have seen less emphasis, and most recently have been largely ignored. Early work by Fenton, et al [10] and later analysis by Ghoshal [11] and Tada, et al [12] show promise but have not as yet led to the development of practical devices. In this paper, a cycle is presented that offers significant improvement in a broad class of solid-state energy conversion devices. The cycle can be used in conjunction with the previously noted improved materials and system designs in which case the benefits compound.

In this presentation, the analysis is described as applied to thermoelectric (TE) devices and systems. Other SSECs, including conventional [6] or tunneling thermionic systems, and with suitable modification, magneto-caloric systems [13] can be utilized.

TE systems have been chosen for illustrative purposes, since their performance is modeled easily, they are well studied and the necessary components to fabricate devices are commercially available from many sources. Thus, experimental systems utilizing the present cycle can be constructed and test results can be compared to theory [15].

Discussion

The common geometry for TE systems used in cooling or heating fluids is shown in Figure 1. Fans (or pumps) pass fluids to be conditioned through heat exchangers on heated and cooled sides of the TE module. The TE module is connected to a suitable source of electric power.

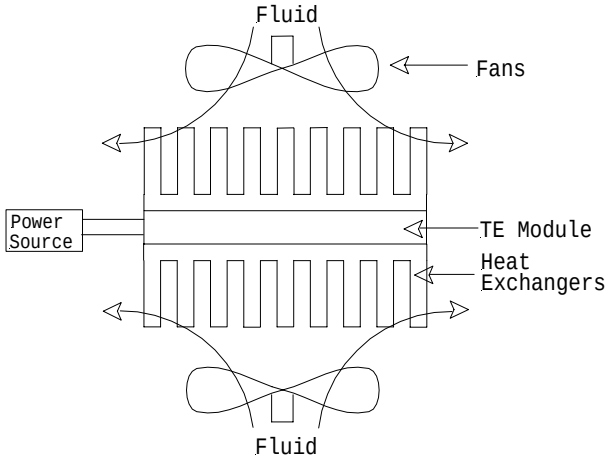

Figure 1.

In this configuration, excluding losses and system inefficiencies, system performance can be computed using well-known formulas [15] that are repeated here for both explanatory purposes and to define terms for the discussion of the thermodynamic cycle that follows.

One side of the TE module is at a higher temperature, T_H , and the other at a lower temperature, T_C. The fluid enters the heat exchangers on both sides of the assembly. Thermal power is transferred to or from the fluid streams.

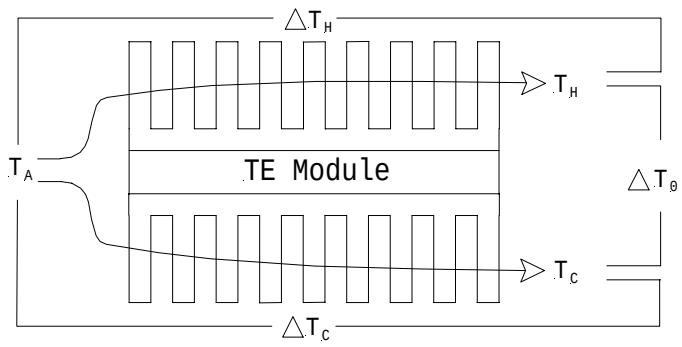

Figure 2.

Referring to Figure 2, for simplicity, it is assumed that both fluids enter at T_A, so that the fluids' temperatures are changed by;

(1) $\Delta T_C = T_A - T_C$

and;

(2) $\Delta T_H = T_H - T_A$

and the total temperature across the TE module is;

(3) $\Delta T_O = \Delta T_H + \Delta T_C$

Here it is assumed properties are temperature independent, the TE element geometry is one dimensional, and current and properties are uniform throughout the plane of the module. For steady-state, the cooling, heating and input powers are given by;

(4) $Q_C = \alpha I(T_A - \Delta T_C) - \frac{1}{2} I^2 R - K\Delta T_O$

(5) $Q_H = \alpha I (T_A + \Delta T_H) + \frac{1}{2} I^2 R - K\Delta T_0$

(6) $Q_{IN} = \alpha I \Delta T_O + I^2 R$

Where;

α = Seebeck Coefficient

I = Current,

R = Electrical Resistance, and

K = Thermal Conductance.

The thermodynamic efficiencies in cooling, ϕ_C, and heating, ϕ_H, are;

(7) $\phi_C = \frac{Q_C}{Q_{IN}}$

(8) $\phi_H = \frac{Q_H}{Q_{IN}}$

And by conservation of energy, for steady-state;

(9) $Q_H = Q_C + Q_{IN}$

So;

(10) $\phi_C + 1 = \phi_H$

Equations (9) and (10) show the interdependence between steady state cooling and heating. In the analysis that follows, the emphasis is placed on cooling. However, using these relations, the results can also be applied to heating.

From Equation (7) using (4) and (6), the current that gives optimum COP is found by maximizing COP with respect to the current I, to yield;

(11) $I_{OPT} = \frac{\alpha \Delta T_O}{R(M-1)}$

Where;

(12) $M = \sqrt{1 + ZT_{AVE}}$

(13) $Z = \frac{\alpha^2}{RK}$

(14) $T_{AVE} = \frac{T_C + T_H}{2}$

And the optimum COP, ϕ_{COPT} is;

(15) $$\phi_{COPT} = \frac{T_C}{\Delta T_O}\left(\frac{M - 1 - \frac{\Delta T_O}{T_C}}{M+1}\right)$$

The first term on the right hand side of Equation (15) is the Carnot cycle efficiency. The term in parenthesis is the fraction of Carnot efficiency for this geometry and material properties characterized by $ZT_{AVE.}$ For the best monolithic Bi Te materials today, $ZT_{AVE} \approx 1$, so for $\frac{\Delta T_0}{T_C} = 0.1;$

(16) $\phi_{COPT} = \frac{T_C}{\Delta T_O} \times 0.130 = 10 \times 0.130 = 1.30 \quad (ZT_{AVE} = 1)$

thus, such TEs under ideal conditions operate at 13% of Carnot (Refrigerant 134 A operates at about 50% of Carnot). Newer materials have the promise of $ZT_{AVE} \approx 2$, so under the same conditions;

(17) $\phi_{COPT} = \frac{T_C}{\Delta T_O} \times 0.228 = 2.28 \quad (ZT_{AVE} = 2)$

or about 23% of Carnot. While materials with a $ZT_{AVE} \approx 2$ result in important efficiency gains, total efficiency remains well below that of two-phase refrigerants.

An alternate geometry and thermodynamic cycle can exhibit higher efficiency gains. Prior to a more general treatment, two examples of the systems that exhibit higher efficiency are discussed. Consider the configuration shown in Figure 3. In this case, the fluids enter from one side. However, the module is constructed so that each TE element (or groups of elements, or individual modules in an assembly of modules) is thermally isolated from its neighbors in the direction of fluid flow and there are effectively an infinite number or a continuum of such elements. Further, each element is in perfect thermal contact with a hot side and a cold side heat exchanger. The heat exchangers themselves are in perfect thermal contact with the fluids and are thermally isolated from their neighbors in the direction of fluid flow. The thermal

conductivity of the fluid in the direction of flow is assumed negligible as is the thermal conductivity of the electrical insulation shown in Figure 3.

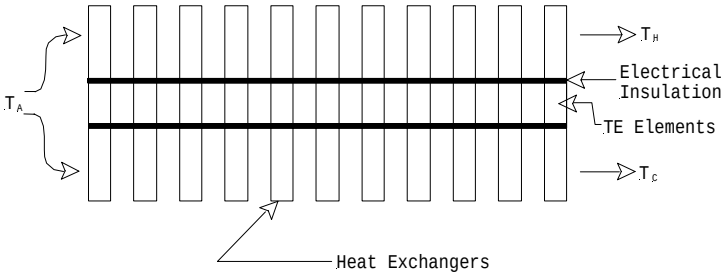

Figure 3.

In this case, the temperature profile of the fluids is shown in Figure 4.

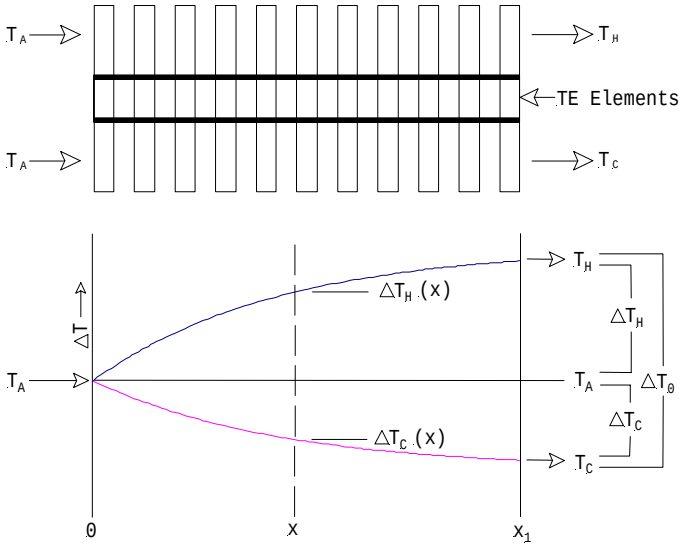

Figure 4.

It is assumed that this is a one-dimensional geometry, with temperatures of the fluids, heat exchangers and TE elements solely a function of *x*, the dimension in the direction of fluid flow. The system spans the length dimension 0 to x_1 and thermal conductivity of the fluid, TE elements and other parts are assumed to be zero in the x direction. Under these conditions the ΔT across each element is;

(18) $$\Delta T(x) = \Delta T_H(x) + \Delta T_C(x)$$

and;

(19) $$0 \le \Delta T(x) \le \Delta T_O,\ 0 \le x \le x$$

for;

(20) $$x < x_1, \Delta T(x) < \Delta T_O$$

But for $\Delta T(x) < \Delta T_O$, from Equation (15), for each element operating at its optimum *COP*; $COP_{COPT}(x) > COP_{COPT}(x_1)$. Thus, the system COP for this configuration can be greater than that of Figure 2 and Equation (15), if the operating condition of each TE element is optimized (or sufficiently close to optimal).

Consider the related geometry of Figure 5 with the same heat transfer conditions, and the one-dimensionality as in Figures 3 and 4.

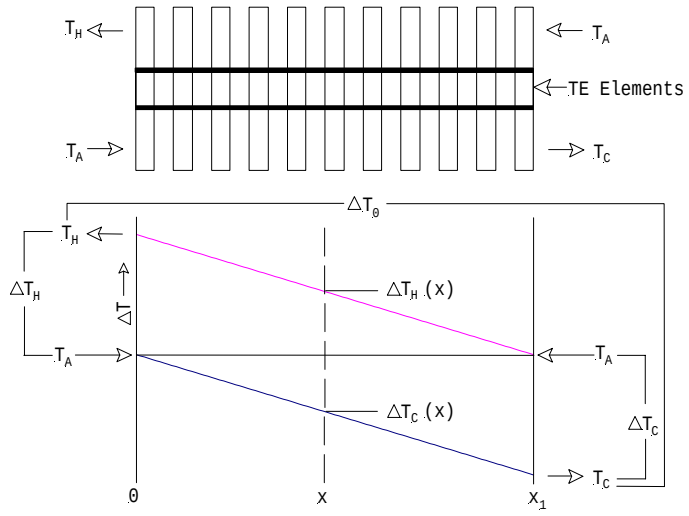

Figure 5.

Consider the case where;

(21) $$\Delta T_C(0) = \Delta T_H(x_1) = 0$$

(22) $$\Delta T_C(x_1) = \Delta T_H(0) = \frac{\Delta T_0}{2}$$

Then, approximately;

(23) $$\Delta T_C(x) + \Delta T_H(x) \approx \frac{\Delta T_O}{2} \text{ for } 0 \le x \le x_1$$

Define $\Delta T_0'$ as;

(24) $$\Delta T_O' \approx \frac{\Delta T_O}{2}$$

Further, the cold side temperature $T_C(x)$ can be approximated by its average $\Delta T_C'$, where;

(25) $$T_C' \approx T_C(0) - \frac{\Delta T_C(x_1)}{2} = T_C(0) - \frac{\Delta T_O}{4}$$

Similarly, *M* becomes M', but;

(26) $$M' = \sqrt{1 + ZT_{AVE}'} \approx \sqrt{1 + ZT_{AVE}} = M$$

Then Equation (15) can be written for this condition to give;

(27) $$\beta_{COPT} \approx \frac{T_C'}{\Delta T_O'}\left(\frac{M' - 1 - \frac{\Delta T_0'}{T_C'}}{M' + 1}\right)$$

which becomes;

(28) $$\beta_{COPT} \approx \frac{2\left(T_C - \frac{\Delta T_O}{4}\right)}{\Delta T_O}\left(\frac{M - 1 - \frac{\Delta T_O}{2(T_C(0) - \frac{\Delta T_O}{4})}}{M+1}\right)$$

For $ZT_{AVE} = 1$ and $\Delta T_O / T_C = 0.1$, $T_{AVE} = T'_{AVE}$;

(29) $$\beta_{COPT} \approx 19.5 \times .1503 = 2.93$$

This is over double the corresponding value for ϕ_{COPT} for the same parameters used in Equation (15).

General Analysis of Isolated Elements Systems

The above cases can be generalized by considering the diagram in Figure 6.

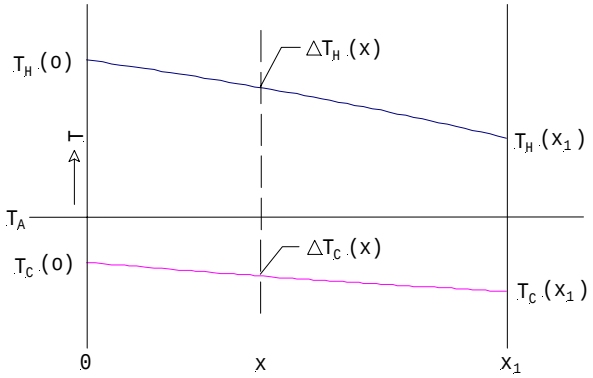

Figure 6.

For fluids flowing with perfect heat transfer to individual TE elements, thermal conductivity in the x direction ignored, and temperature independent properties, Equations (4), (5), and (6) can be written at each position in terms of the heat transfer to the fluid as;

(30) $$q_C(x) = M_C C_{PC} \frac{d\Delta T_C(x)}{dx}$$

(31) $$= \frac{1}{x_1}\left[\alpha I(x)(T_C(0) - \Delta T_C(x)) - \frac{I^2(x)R(x)}{2} - K(x)\Delta T(x)\right]$$

(32) $$q_H(x) = M_H C_{PH} \frac{d\Delta T_H(x)}{dx}$$

(33) $$= \frac{1}{x_1}\left[\alpha I(x)(T_H(0) + \Delta T_H(x)) + \frac{I^2(x)R(x)}{2} - K(x)\Delta T(x)\right]$$

(34) $$q_{IN}(x) = \frac{1}{x_1}\left[\alpha I(x)\Delta T(x) + I^2(x)R(x)\right]$$

Here I, R and K are assumed to vary with x. M_C and M_H are the cold and hot side fluid flow rates and C_{PC} and C_{PH} are their corresponding heat capacities.

Consider simplifying the Equations (31), (33), and (34) so that at every position x, all TE elements are operating at the same proportion of the current that gives optimum *COP*,
then;

(35) $$I(x) = \in I_{OPT}(x)$$

Further, assume that;

(36) $$M(x) = \sqrt{1 + ZT_{AVE}(x)} \approx \sqrt{1 + ZT_{AVEO}}$$

and T_{AVEO} is the average temperature of all elements. This assumption introduces acceptable error for cooling and heating since (1) the average temperature of any individual element is not likely to differ more than 10% from a system average, (2) the induced errors will tend to compensate when averaged over the entire system, (3) the error for COP is small for changes in I near the optimum, and (4) the approximation is conservative in that it slightly underestimates the calculated *COP*. With this approximation, and noting that if *R(x)* is set equal to;

(37) $$R(x) = \frac{R(x_1)\Delta T(x)}{\Delta T_O} = \frac{R_O \Delta T(x)}{\Delta T_O}$$, where $R(x_1) = R_O$

then;

(38) $$I(x) = \in I_{OPT} = \in I_0$$

which is independent of *x*.

The interdependence of *R(x)* and *K(x)*, for *Z (*which is assumed to be independent of position) yields;

(39) $$Z = \frac{\alpha^2}{R(x)K(x)} = \frac{\alpha^2 \Delta T_O}{R_O \Delta T(x) K(x)}$$

So;

(40) $$K(x) = \frac{\alpha^2 \Delta T_O}{R_O Z \Delta T(x)} = \frac{K_O \Delta T_O}{\Delta T(x)}$$ with $$K(x_1) = K_O = \frac{\alpha^2}{R_O Z}$$

Thus, the product;

Using these values for *I*, *R*, and *K* in Equations (31), (33) and (34);

(41) $$q_C(x) = \frac{1}{x_1}\left[\alpha I_O \in (T_C(0) - \Delta T_C(x)) - \frac{I^2{}_O \in^2 R_O}{2}\frac{\Delta T(x)}{\Delta T_O} - K_O \Delta T_O\right]$$

(42) $$q_H(x) = \frac{1}{x_1}\left[\alpha I_O \in (T_H(0) + \Delta T_H(x)) + \frac{I^2{}_O \in^2 R_O}{2}\frac{T(x)}{\Delta T_O} - K_O \Delta T_O\right]$$

(43) $$q_{IN}(x) = \frac{1}{x_1}\left[\alpha I_O \in \Delta T_0 + I^2{}_O \in^2 R_O\right]\frac{\Delta T(x)}{\Delta T_O}$$

Let;

(44) $$\theta_C(x) = \frac{\Delta T_C(x)}{\Delta T_O}$$, $$\theta_H(x) = \frac{\Delta T_H(x)}{\Delta T_O}$$, and $$\theta(x) = \frac{\Delta T(x)}{\Delta T_O}$$

Then substituting the dimensionless temperatures defined in Equations (44) into (30), (32), (41), (42), and (43);

(45) $$\theta'_C(x) = \frac{q_C}{C_{PC} M_C \Delta T_O}$$

(46)

$$= \frac{1}{C_{PC} M_C \Delta T_O x_1} \left[\alpha I_O \in T_C(0) - K_O \Delta T_O - \alpha I_O \in \Delta T_O \theta_C(x) - \frac{I_O^{\,2} \in^2 R_O}{2} \theta\ (x) \right]$$

(47) $$= A_C + B_C \theta_C(x) + C_C \theta\ (x)$$

(48) $$\theta_H'(x) = \frac{q_H}{C_{PC} M_H \Delta T_O}$$

(49)

$$= \frac{1}{C_{PH} M_H \Delta T_O x_1} \left[\alpha I_O \in T_H(0) - K_O \Delta T_O + \alpha I_O \in \Delta T_O \theta_H(x) + \frac{I^2{}_O \in^2 R_O}{2} \theta\ (x) \right]$$

(50) $$= A_H + B_H \theta_H(x) + C_H \theta\ (x)$$

(51) $$q_{IN}(x) = (\alpha I_O \in \Delta T_O + I_O^{\,2} \in^2 R_O) \frac{\theta\ (x)}{x_1}$$

(52) $$= A_H - A_C + B_H \theta_H(x) - B_C \theta_C(x) + (C_H - C_C) \theta\ (x)$$

where;

(53) $$A_C = \frac{\alpha I_O \in T_C(0) - K_O \Delta T_O}{C_{PC} M_C \Delta T_O x_1}$$

(54) $$B_C = -\frac{\alpha I_O \in}{C_{PC} M_C x_1}$$

(55) $$C_C = -\frac{I_0^{\,2} \in^2 R_O}{2 C_{PC} M_C \Delta T_O x_1}$$

(56) $$A_H = \frac{\alpha I_O \in T_H(0) - K_O \Delta T_O}{C_{PH} M_H \Delta T_O x_1}$$

(57) $$B_H = \frac{\alpha I_O \in}{C_{PH} M_H x_1}$$

(58) $$C_H = \frac{I_O^{\,2} \in^2 R_O}{2 C_{PH} M_H \Delta T_O x_1}$$

Equations (47) and (50) can be separated to yield;

(59) $$0 = \theta_C'' + D\theta_C' + E\theta_C + F_C$$

(60) $$0 = \theta_H'' + D\theta_H' + E\theta_H + F_H$$

where;

(61) $$D = -\left(B_C + C_C + B_H + C_H\right)$$

(62) $$E = (B_C + C_C)(B_H + C_H) - C_C C_H$$

(63) $$F_C = -A_H C_C + A_C (B_H + C_H)$$

(64) $$F_H = -A_C C_H + A_H (B_C + C_C)$$

The solutions for Equations (59) and (60) are as expected;

(65) $$\theta_C(x) = \frac{-F_C}{E} + C_{1C} e^{R_1 x} + C_{2C} e^{R_2 x}$$

(66) $$\theta_H(x) = \frac{-F_H}{E} + C_{1H} e^{R_1 x} + C_{2H} e^{R_2 x}$$

where;

(67) $$R_1 = -\frac{D + \sqrt{D^2 - 4E}}{2}$$

(68) $$R_2 = -\frac{D - \sqrt{D^2 - 4E}}{2}$$

(69) $$C_{1C} = \frac{\theta_C(x_1) - \theta_C(0) e^{R_2 x_1} + \frac{F_C}{E}(1 - e^{R_2 x_1})}{e^{R_1 x_1} - e^{R_2 x_1}}$$

(70) $$C_{2C} = \frac{-\theta_C(x_1) + \theta_C(0) e^{R_1 x_1} - \frac{F_C}{E}(1 - e^{R_1 x_1})}{e^{R_1 x_1} - e^{R_2 x_1}}$$

(71) $$C_{1H} = \frac{\theta_H(x_1) - \theta_H(0) e^{R_2 x_1} + \frac{F_H}{E}(1 - e^{R_2 x_1})}{e^{R_1 x_1} - e^{R_2 x_1}}$$

(72) $$C_{2H} = \frac{-\theta_H(x_1) + \theta_H(0) e^{R_1 x_1} - \frac{F_H}{E}(1 - e^{R_1 x_1})}{e^{R_1 x_1} - e^{R_2 x_1}}$$

The *COP* in cooling defined in Equations (7) and (10) can be written as the ratio of the cooling power to the input power;

(73) $$\beta_C = \frac{\int_0^{x_1} q_C(x) dx}{\int_0^{x_1} q_{IN}(x) dx}$$

and the thermal cooling power out to the net power in, from Equation (9) and the first integral of Equations (45) and (48) for the cooling and heating powers, respectively;

(74) $$\beta_C = \frac{\Delta\theta_C}{\frac{C_{PH} M_H}{C_{PC} M_C} \Delta\theta_H - \Delta\theta_C}$$

where;

(75) $$\Delta\theta_C = \theta_C(x_1) - \theta_C(0)$$

(76) $$\Delta\theta_H = \theta_H(x_1) - \theta_H(0)$$

Equation (73) can be written explicitly using Equations (41) and (43) in a form similar to Equation (51);

(77) $$q_C(x) = \frac{1}{x_1}(\alpha I_O \in (T_A - \Delta T_0\theta_C(x) - \frac{I^2{}_O \in^2 R_O}{2}\theta(x) - K_O\Delta T_O)$$

(78) $$q_{IN}(x) = \frac{1}{x_1}(\alpha I_O \in \Delta T_O + I_O{}^2 \in^2 R_O)\theta(x)$$

Then if $Q_{C\beta}$ and $Q_{IN\beta}$ are defined as the total cooling power and power in, respectively;

(79) $$Q_{C\beta} = \int_0^{x_1} q_C(x)dx$$

(80) $$Q_{IN\beta} = \int_0^{x_1} q_{IN}(x)dx$$

Using Equations (77), (78), (79) and (80) in (73) the *COP*, β_C, becomes;

(81) $$\beta_C = \frac{\alpha I_O \in T_A - K_O\Delta T_O - \alpha I_O \in \Delta T_0 \int_0^{x_1}\frac{\theta_C(x)}{x_1}dx - \frac{I_O{}^2\varepsilon^2 R_O}{2}\int_0^{x_1}\frac{\theta(x)}{x_1}dx}{(\alpha I_O \in \Delta T_O + I_O{}^2 \in^2 R_O)\int_0^{x_1}\frac{\theta(x)}{x_1}dx}$$

After substituting Equation (11) for I_O, Equations (79) and (80) can be written in terms of Z as;

(82) $$Q_{C\beta} = K_0\Delta T_0\left[\frac{ZT_A \in}{(M-1)}\left(1 - \frac{\Delta T_0}{T_A}\left(\int_0^{x_1}\frac{\theta_C(x)}{x_1}dx + \frac{\in}{2(M-1)}\int_0^{x_1}\frac{\theta(x)}{x_1}dx\right)\right) - 1\right]$$

(83) $$Q_{IN\beta} = K_0\Delta T_0\left[\frac{ZT_A \in}{(M-1)}\left(\frac{\Delta T_0}{T_A} + \frac{\in}{(M-1)}\right)\int_0^{x_1}\frac{\theta(x)}{x_1}dx\right]$$

So that Equation (81) becomes;

(84) $$\beta_C = \frac{1 - \frac{\Delta T_0}{T_A}\left(\int_0^{x_1}\frac{\theta_C(x)}{x_1}dx + \frac{\in}{2(M-1)}\int_0^{x_1}\frac{\theta(x)}{x_1}dx\right) - \frac{(M-1)}{ZT_A \in}}{\left(\frac{\Delta T_0}{T_A} + \frac{\in}{(M-1)}\right)\int_0^{x_1}\frac{\theta(x)}{x_1}dx}$$

The *COP*, ϕ_C, for the equivalent standard device with the same α, $\in$, R_0, K_0, T_C (0), and ΔT_0 (thus Z is the same and *M* is approximated as the same);

(85) $$\phi_C = \frac{Q_{C\phi}}{Q_{IN\phi}}$$

Where $Q_{C\phi}$ and $Q_{IN\phi}$ are derived from Equations (4) and (6) with substitutions the same as those of Equations (82) and (83), but the parameters are independent of x;

(86) $$Q_{C\phi} = K_0\Delta T_0\left[\frac{ZT_A \in}{(M-1)}\left(1 - \frac{\Delta T_0}{T_A}\left(1 + \frac{\in}{2(M-1)}\right)\right) - 1\right]$$

(87) $$Q_{IN\phi} = K_0\Delta T_0\frac{ZT_A \in}{(M-1)}\left(\frac{\Delta T_0}{T_A} + \frac{\in}{(M-1)}\right)$$

The ratio $\frac{\beta_C}{\phi_C}$ can be written using Equations (84), (85), (86) and (87);

(88) $$\frac{\beta_C}{\phi_C} = \frac{1 - \frac{\Delta T_0}{T_A}\left(\int_0^{x_1}\frac{\theta_C(x)}{x_1}dx + \frac{\in}{2(M-1)}\int_0^{x_1}\frac{\theta(x)}{x_1}dx\right) - \frac{(M-1)}{ZT_A \in}}{\left(1 - \frac{\Delta T_0}{T_A}\left[1 + \frac{\in}{2(M-1)}\right] - \frac{(M-1)}{ZT_A \in}\right)\int_0^{x_1}\frac{\theta(x)}{x_1}dx}$$

This ratio, $\frac{\beta_C}{\phi_C}$, will be used as the main comparison between the efficiencies of the present and conventional TE systems.

The solutions presented above give means to compute both cold side and hot side temperature profiles and the corresponding *COPs*. Thus, in addition to the cooling results discussed here, the analysis is useful for heating as well.

Four special cases are of interest. These cases show several important characteristics of the present thermodynamic cycle. The computations are simplified by selecting appropriate boundary conditions and introducing suitable approximations.

Case 1: $\theta_C(0) = 0$; and $\theta_H(x) \equiv 0$ (the hot side is an infinite heat sink). Since $\theta_H(x) \equiv 0$, $\theta(x) = \theta_C(x)$. For these conditions, Equation (82) can be written as;

(89) $$Q_{C\beta} = K_0\Delta T_0\left[\frac{ZT_A \in}{(M-1)}\left(1 - \frac{\Delta T_0}{T_A}\left(1 + \frac{\in}{2(M-1)}\right)\int_0^{x_1}\frac{\theta(x)}{x_1}dx\right) - 1\right]$$

and Equation (83) remains the same since here $\theta_C(x) = \theta(x)$. Thus the *COP*, β_C, for this case becomes;

(90) $$\beta_C = \frac{1 - \frac{\Delta T_0}{T_A}\left(1 + \frac{\in}{2(M-1)}\right)\int_0^{x_1}\frac{\theta(x)}{x_1}dx - \frac{(M-1)}{ZT_A \in}}{\left(\frac{\Delta T_0}{T_A} + \frac{\in}{(M-1)}\right)\int_0^{x_1}\frac{\theta(x)}{x_1}dx}$$

And $\frac{\beta_C}{\phi_C}$ becomes;

(91) $$\frac{\beta_C}{\phi_C} = \frac{1-\frac{\Delta T_0}{T_A}\left(1+\frac{\in}{2(M-1)}\right)\int_0^{x_1}\frac{\theta(x)}{x_1}dx - \frac{(M-1)}{ZT_A\in}}{\left(1-\frac{\Delta T_0}{T_A}\left[1+\frac{\in}{2(M-1)}\right]-\frac{(M-1)}{ZT_A\in}\right)\int_0^{x_1}\frac{\theta(x)}{x_1}dx}$$

Since $\theta_H(x)\equiv 0$, Equation (47) for $\theta_C(x)$ becomes a first order linear differential equation. Its solution is;

(92) $$\theta(x) = \frac{-A_C}{B_C + C_C}\left(1-e^{(B_C+C_C)x}\right)$$

Using the boundary conditions $\theta(0)=0$, $\theta(x_1)=1$; the integral in Equations (89), (90) and (91) is found to be;

(93) $$\int_0^{x_1}\frac{\theta(x)}{x_1}dx = \ln^{-1}\left(1+\frac{B_C+C_C}{A_C}\right)-\frac{A_C}{B_C+C_C}$$

When Equations (53), (54), and (55) are combined in the form found in Equation (93), $C_{PC}M_C$ is eliminated and;

(94) $$\frac{A_C}{B_C+C_C} = \frac{-T_A}{\Delta T_0}\left(\frac{1-\frac{(M-1)}{ZT_A\in}}{1+\frac{\in}{2(M-1)}}\right)$$

Equations (93) and (94) can be used to evaluate into Equation (91). Figure 7 is a plot of β_C/ϕ_C as a function of $\frac{\Delta T_O}{\Delta T_{MAX}}$, for $ZT_A = 1$ and several values of $\in$, where;

(95) $$\Delta T_{MAX} = \frac{ZT_C{}^2}{2}$$

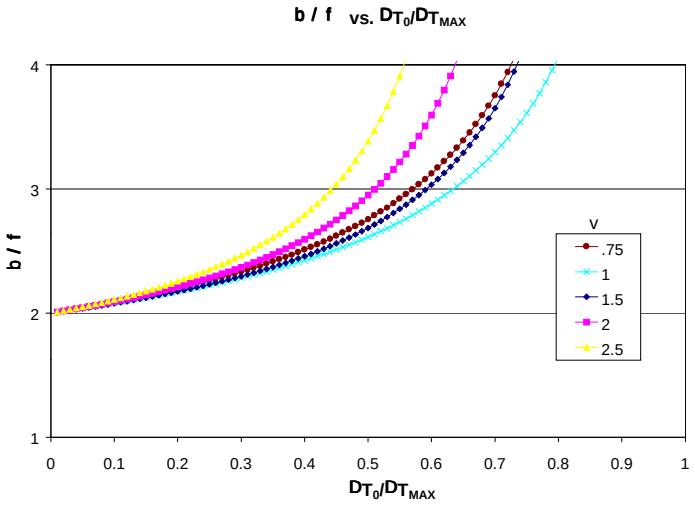

Figure 7.

Figure 8 is the temperature profile as a function of $\frac{x}{x_1}$, for several values of ZT_A, a constant ΔT_0 of 45^0K, and $T_A = 300^0$K.

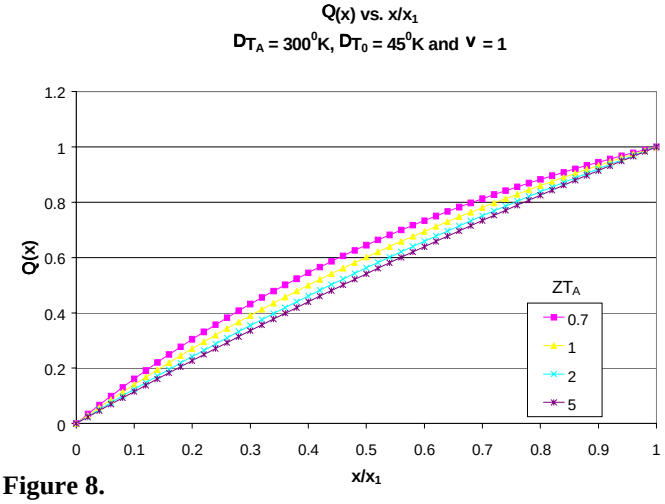

Figure 8.

Figure 8 suggests that $\theta(x)$ can be approximated by;

(96) $$\theta(x) \approx \frac{x}{x_1} \text{ for } \frac{\Delta T_O}{\Delta T_{MAX}} << 1,$$ that is, for ΔT_O small compared to the maximum possible temperature change in cooling, ΔT_{MAX}.

Using Equation (96) in the integrals in Equation (91);

(97) $$\frac{\beta_C}{\phi_C} \approx 2+\frac{\Delta T}{T_A}\left(1+\frac{\in}{2(M-1)}\right)\phi_C{}^{-1} \qquad \Delta T_O \le \frac{\Delta T_{MAX}}{2}$$

$\theta_C(0)=0$, infinite heat sink.

Case 2: $\theta_C(0)=\theta_H(0)=0; \quad \theta_C(x_1)=\theta_H(x_1)=\frac{1}{2}$

The conditions for this case are those shown qualitatively in Figure 4, but with the hot and cold side dimensionless temperatures each equal to ½, and the inlet temperatures equal to zero.

Note that for these boundary conditions, Equations (69-72) reduce to

(98) $$C_{1C,H} = \frac{\frac{1}{2}+\frac{F_{C,H}}{E}(1-e^{R_2x_1})}{e^{R_1x_1}-e^{R_2x_1}}$$

(99) $$C_{2C,H} = \frac{-\frac{1}{2} - \frac{F_{C,H}}{E}(1 - e^{R_1 x_1})}{e^{R_1 x_1} - e^{R_2 x_1}}$$

Where;

(100) $$F_c = -F_H$$

and the order of the subscripts C, H is preserved on both sides of Equations (98) and (99).

Then, Equation (74) becomes;

(101) $$\beta_C = \frac{1}{\frac{C_{PH} M_H}{C_{PC} M_C} - 1}$$

as expected. Integration of both sides of Equations (47) and (50) yield $\theta_C(x_1) - \theta_C(0)$ and $\theta_H(x_1) - \theta_H(0)$ as a function of Equations (98) and (99) and the variables in Equations (53-58). By simultaneously numerically solving Equations (47) and (50) for $C_{PC} M_C$ and $C_{PH} M_C$, β_C in Equation (101) can be computed. That result divided by the value for ϕ_C from Equations (85-87) with the same conditions yields β_C / Q_C for this case.

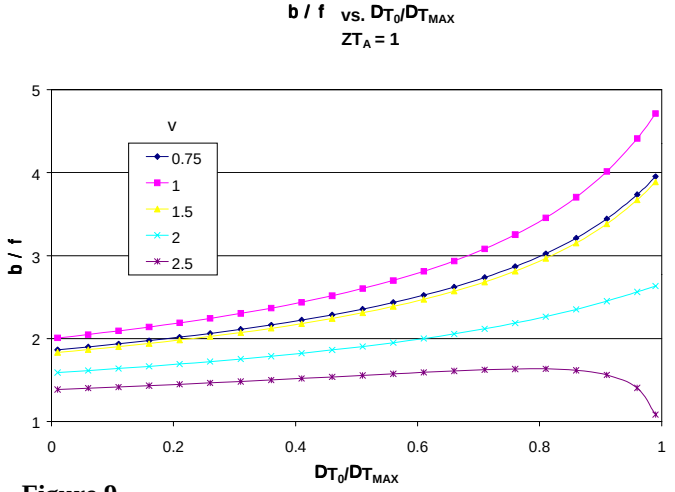

Figure 9.

Figure 9 presents β_C / ϕ_C as a function of $\frac{\Delta T_O}{\Delta T_{MAX}}$ for various values of $\in$ with $ZT_A = 1$, and Figure 10 for $\in = 1$ and ZT_A varying.

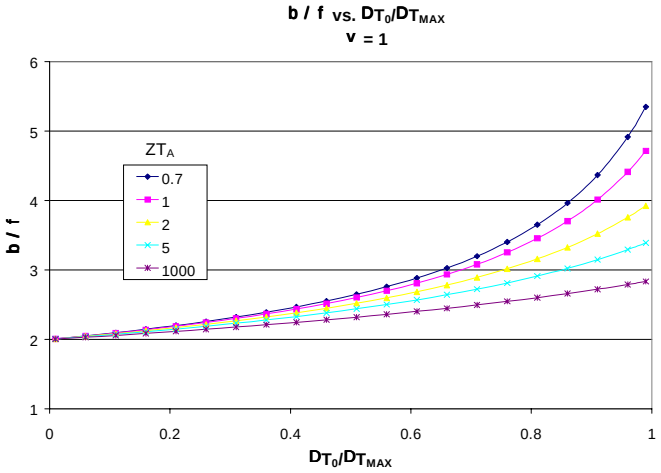

Figure 10.

Case 3: $\theta_C(0) = \theta_H(x_1) = 0$; $\theta_C(x_1) = \theta_H(0) = 1$.
This is a counter flow system of the type shown in Figure 6. The temperature profiles are found from Equations (65) and (66), using the boundary conditions for this case. The coefficients are;

(102) $$C_{1C} = \frac{1 + \frac{F_C}{E}(1 - e^{R_2 x_1})}{e^{R_1 x_1} - e^{R_2 x_1}}$$

(103) $$C_{2C} = \frac{-1 - \frac{F_C}{E}(1 - e^{R_1 x_1})}{e^{R_1 x_1} - e^{R_2 x_1}}$$

(104) $$C_{1H} = \frac{-e^{R_2 x_1} + \frac{F_H}{E}(1 - e^{R_2 x_1})}{e^{R_1 x_1} - e^{R_2 x_1}}$$

(105) $$C_{2H} = \frac{e^{R_1 x_1} - \frac{F_H}{E}(1 - e^{R_1 x_1})}{e^{R_1 x_1} - e^{R_2 x_1}}$$

The numerical process described in Case 3 can then be used to compute $C_{PC} M_C$, $C_{PH} M_H$ and other functions. Plots of $\theta_C(x)$ and $\theta_H(x)$ for 3 values of $\frac{\Delta T_O}{\Delta T_{MAX}}$ and $ZT_A = 1$ are presented in Figure 11. The Figure shows the near linear shape of the temperature profiles and suggests that a linear approximation, such as that in Equation (28), is quite useful.

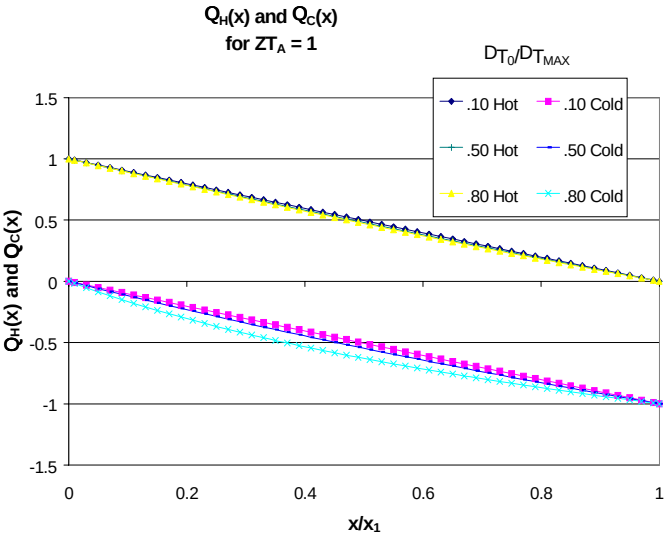

Figure 11.

Figure 12 gives the error E_β of the approximate solution (linear $\theta_C(x)$ and $\theta_H(x)$) for the maximum $COP, \in = 1)$ compared to the numerical solution to Equation (91), for the boundary conditions for this case and representative values of ZT_A.
Here;

(106) $$E_\beta = \frac{\beta - \beta_A}{\beta}$$

and β_A is given by Equation (28);

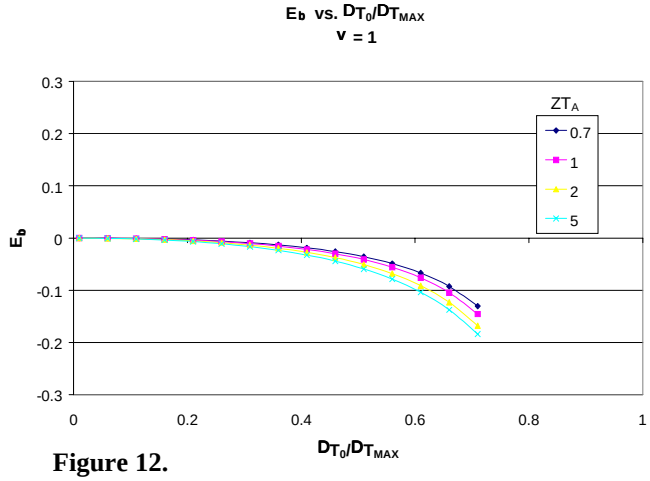

Figure 12.

Figure 13 gives the numerical solution for β/ϕ as a function of $\frac{\Delta T_O}{\Delta T_{MAX}}$, for several values of $\in$ and $ZT_A = 1$.

.

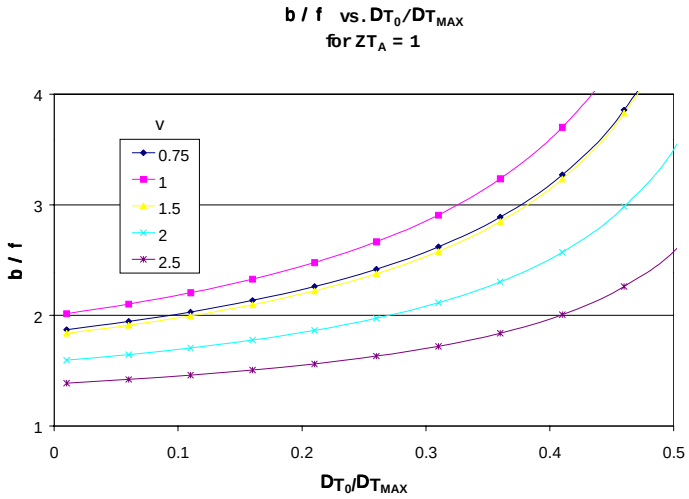

Figure 13.

Case 4: $\theta_C(0) = \theta_H(x_1) = r,\ \theta_C(x_1) = \theta_H(0) = 1$
The improvement in performance (β/ϕ) is a function of the difference between the fluid inlet temperatures $\theta_C(0)$ and $\theta_H(x_1)$ and the respective outlet temperatures. Figure 14 gives examples, for the outlet temperatures, $\theta_C(X_1) = \theta_H(0) = 1$, with temperature profiles for $\theta_C(0) = \theta_H(1) = R$. The $R = 0$ profiles correspond to Case 3. The profiles with $R = 0.5$ have incoming fluids at temperatures substantially different from ambient and represent an intermediate condition. Profiles with $R = 0.95$ are the extreme where $\theta_C(0)$ approaches $\theta_C(x_1)$ and $\theta_H(x_1)$ approaches $\theta_H(x_1)$ so that the fluid experiences very little temperature changes while passing through the TE system.

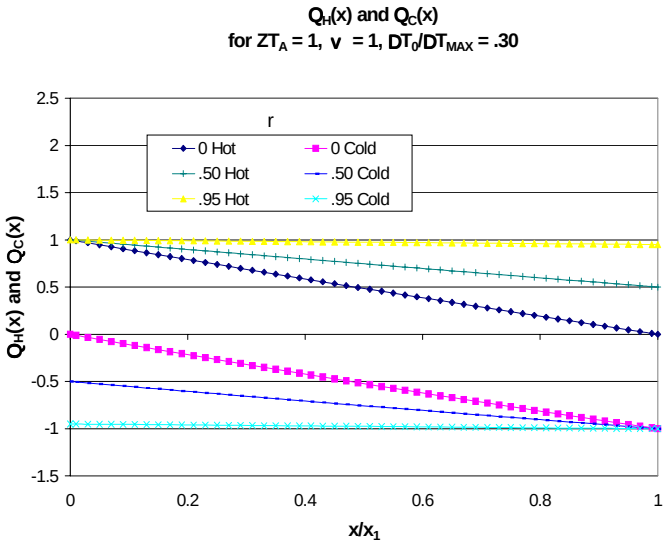

Figure 14.

Figure 15 presents β/ϕ several values of r with $\in = 1$ and $ZT_{AVE} = 1$. Notice that as r approaches 1, that is, as that the inlet and outlet temperatures approach equality, β/ϕ approaches 1 so the gain in performance diminishes

to zero. In figure 15, the range of $\frac{\Delta T_O}{\Delta T_{MAX}}$ is from 0 to 0.5.

In the graph, ΔT_{MAX} is the maximum value for r = 0. This condition, r = 0, corresponds to systems such as air conditioners with 100% air uptake, Amerigon's CCS system, personal coolers and electronic equipment air convection cooling systems.

The condition $r \approx 1$ corresponds to conditions in refrigerators, cold boxes and certain on-chip semi-conductor coolers in which heat sinking is done directly. Automotive, home and industrial HVAC systems typically operate with $r \approx 0.2$ to 0.6.

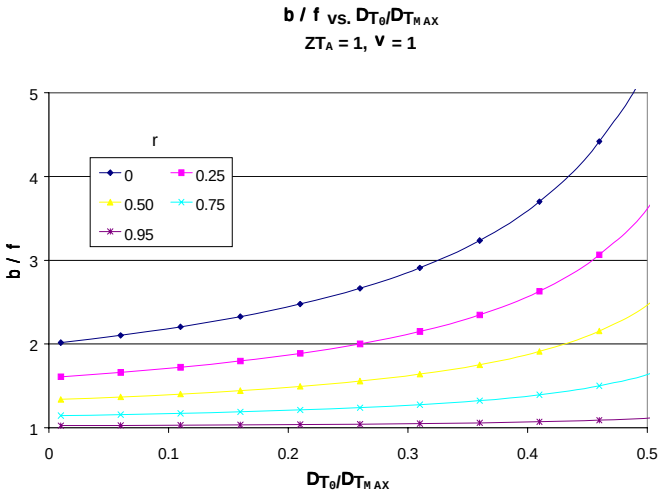

Figure 15.

Summary and Conclusions

A quite general analysis of an alternate solid-state cycle has been developed. It has been discussed above in its application to thermoelectric systems and cooling in particular. Nevertheless, the results are applicable to heating, and to thermionics, magneto-caloric, and related solid-state energy converters. Such solid-state systems are similar in that their designs can be optimized quite readily at the component level throughout typical performance ranges, since power is transferred and conditioned by simple electrical and mechanical componentry. In contrast, such optimization of two-phase systems requires valves, pumps and the like to be segregated into multiple flow segments, thereby introducing substantial complexity to the mechanical componentry.

Results for the present cycle are given for several cases of practical interest and also for more general systems. The analyses show that for systems that can utilize convective thermal power transport, and have fluid temperature changes that are a substantial fraction of the outlet temperature, performance is about a factor two times that of traditional solid-state systems. In addition, with counter flow in thermoelectric systems, such as in Case 3, the total temperature difference between the cold and hot side fluids at the outlets is a factor of 2 higher than that for a conventional TE counterpart. Thus the performance range is extended to temperature differentials otherwise only possible with cascade configurations, and their attendant very low COPs. This advantage can be significant for systems requiring high temperature differentials, or high thermal fluxes.

The advantages of the present cycle are summarized qualitatively in Figure 16, which depicts typical cooling power curves for TE systems. Curve S_1, is for standard TE module (equivalent to r = 1 in the terminology of this paper). Curve S_2 is for the present system with r = 0. Point P_1, is a hypothetical required operating condition. It can be seen that the proposed system can deliver a higher Q_C (point P_2) at the same ΔT_{C1}, or a substantially larger ΔT_{C2} for the same Q_C (point P_3). Alternately the power input can be reduced while the specified Q_C and ΔT combination is maintained. Notice, however, that if the system under consideration had $r \approx 1$, curve S_2 would move to coincide with S_1, and there would be no performance gain using the proposed system.

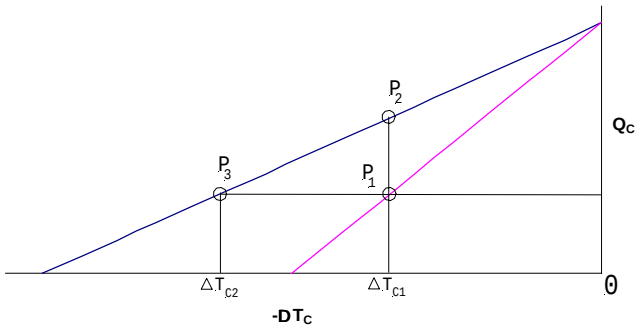

Figure 16.

This analysis assumes that the TE material can be described as a continuum. In practical systems this will not be the usual case. It is necessary to understand how results differ for a finite number of isolated units from those presented in this paper. Unpublished detailed simulations of various numbers of elements that result in effective thermal isolation show that even though significant gains in efficiency occur for a small number of isolated units (i.e. 2-5), the number must be quite large (i.e. 35-70) to approach theoretical maximum performance. Since in practical devices, the number of elements is often over 100, this does not generally present a significant limitation, and with due care, present analysis can be used as an approximation.

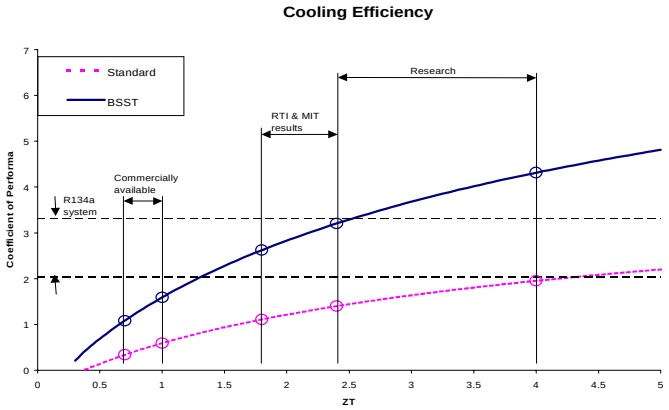

Figure 17.

The above discussion is presented in terms of moving working fluids. This represents a limitation for certain applications, but for applications that require the cooling and/or heating of fluids, it is generally not at all limiting since the fluids require movement as part of their basic function. For other applications and geometries, movable solid thermal conductors can replace the fluids discussed here. Generally, performance is enhanced in systems that use highly conductive solids if the solid moving members are anisotropic, so as to have reduced thermal conductivity in the direction of motion.

As a final comment, thermoelectric systems with very high aspect ratio (thickness to area) thermoelectric elements can have sufficient isolation perpendicular to the direction of current flow, that the effect can be expressed and utilized at the element level.

The present cycle is compatible with materials of arbitrary *ZT*. Figure 17 shows *COP* as a function of ZT_{AVE} for the various values of *r*. The horizontal band represents the *COP* for *R134A* for a typical automotive HVAC system. Under the same conditions $\Delta T = 30^{\circ}C$, $T_C = 280^{\circ}K$, the curves show the values of ZT_{AVE} for which performance is equivalent. Indicated by vertical lines are ranges of *ZT* for present RTI and MIT materials [1, 2], and possible future materials. The combination of the present cycle with the emerging new materials is expected to allow the development of solid-state systems with performances competitive with those of present two-phase heating, cooling and ventilation systems.

Acknowledgments

The author is indebted to several colleagues: Mr. R. Diller for reviewing simulations and conducting experiments; Mr. Y. Chang for conducting experiments; Ms. J. Garcia for document preparation; Mr. A. Nannini for doing numerical simulations and proof reading, and Dr. C. Vining for review and comment.

References

1. Venkatasubramanian, R. *et al*, "Thin-Film Thermoelectric Devices With High Room-Temperature Figures Of Merit," *Nature*, Vol. 413, (2001), pp. 597-602.

2. Harman, T.C., oral presentation, DARPA/ONR/DOE Thermoelectric Workshop, San Diego, CA, U.S.A., (2002).

3. Nolas, G., *et al.*, Thermoelectric Materials 2002—Research and Applications, Materials Research Society, (Warrensdale, PA, 2002), pp. 269-274.

4. Ghamaty, S. *et al*, "Development of Quantum Well Thermoelectric Device,"*Proc.18th Int. Conf. On Thermoelectrics, ICT'99*, San Diego, CA, U.S.A., (1999).

5. Nolas, G. S., Kaeser, M., Littleton, R. T., and Tritt, T Skutterudite Materials,"*Appl. Phys. Letter*, Vol. 77, No. 12, (2000), pp. 1855-1857.

6. Shakouri, A., *et al*, "Heterostructure Integrated Thermionic Coolers," *Appl. Phys. Letter71*, (9), (1997), pp. 1234-1236.

7. Nolas, G., *et al.*, Thermoelectrics Basic Principles and New Materials Developments, Springer (Berlin), pp.151-162.

8. Kishi, M., *et al.*, "Fabrication of a miniature thermoelectric module with elements composed of sintered Bi-Te compounds," *Proc 16th Int. Conf. On Thermoelectrics*, Dresden, GERMANY, 1997, pp. 653-663.

9. Hydrocool Pty Ltd., "Enhanced Thermoelectric Refrigeration System COP, Through Low Thermal Resistance Liquid Heat Transfer System," *Proc ICT '98 Conf.*, Nagoya, JAPAN, 1998, pp. 1-9.

10. Fenton, J. W, *et al*, "Counter-Flow Thermoelectric Heat Pump with Discrete Sections," United States Patent No. 4,065,936, (1978).

11. Ghoshal, U., "Thermoelectric Cooling with Plural Dynamic Switching to Isolate Heat Transport Mechanisms," United States Patent No. 5,867,990, (1999).

12. Tada, S., *et al*, "A New Concept of Porous Thermoelectric Module Using a Reciprocating Flow for Cooling/Heating System (Numerical Analysis for Heating System)," *Proc 16th Int. Conf. On Thermoelectrics*, Dresden, GERMANY, 1997, pp. 664-667.

13. Pecharsky, V. K., *et al.*, "Tunable Magnetic Regenerator Alloys with a Giant Magneto caloric Effect for Magnetic Refrigeration from ~20 to ~290K," *Appl. Phys. Letter 70*, (24), (1997), pp. 3299-3301.

14. Goldsmid, H.J., Electronic Refrigeration, Page Bros (Norwich) Limited (Great Britain, 1986).